Int. J. Heat Mass Transfer. Vol. 14, pp. 793–812. Pergamon Press 1971. Printed in Great Britain

THE STEADY EVAPORATION AND MIXING OF A SPRAY IN A GASEOUS SWIRL

D. ADLER* and W. T. LYN†

King's College, University of London, England

(*Received* 2 *January* 1970 *and in revised form* 17 *July* 1970)

Abstract—A theory for the calculation of the steady evaporation and mixing of a liquid spray in a gaseous swirl is described and backed by a number of experiments. This theory is based on continuum mechanics rather than on single droplet theory thus allowing proper consideration of the interaction between the droplets within the spray.

The path of the spray, rate of evaporation as well as concentration velocity and temperature fields, can be calculated.

The resulting equations must be solved numerically. Thus discussions of the numerical procedure and of the numerical investigation of the equations are given.

NOMENCLATURE

A, surface area of a drop;

b, width of the spray (Fig. 1);

C, $= f_c\phi_c c_{mo}\kappa C_L + f_c\phi_c c_{mo}(1-\kappa)\,C_{pv} + (1 - f_c\phi_c c_{mo})\,C_{pg}$, specific heat of the mixture;

c, concentration;

c_b, coefficient in equation (17);

C_d, $= k_D R'_e$, drag coefficient of a droplet [11];

C_{de}, deflection coefficient;

C_L, specific heat of the liquid;

C_p, specific heat at constant pressure;

C_{pv}, specific heat of the vapour;

C_{T1}, $= (C_L - C_{pg})\,T_{eq}$;

C_{T2}, $= \dfrac{\rho_{mo} T_{eq}}{\Delta T_{mo}}$;

C_ρ, a coefficient in the density ratio of appendix 1, section C, representing the assumed evaporation rate;

D, diffusion coefficient;

d_{sa}, mean Sauter diameter of the spray;

F_c, centrifugal force acting on a spray element;

F_g, deflecting gas force acting on a spray element;

f, universal similarity profile inside the spray;

f_{C_p}, $= C/C_L$;

f_ρ, $= \rho/\rho_{mo}$;

H, latent heat of evaporation;

h, film heat-transfer coefficient in absence of mass transfer;

$I_{c\rho}$, $= \int_{-1}^{1} f_c f_\rho \,d\xi$;

$I_{T\rho C_p}$, $= \int_{-1}^{1} f_T f_\rho f_{C_p} \,d\xi$;

$I_{vc\rho}$, $= \int_{-1}^{1} f_v f_c f_\rho \,d\xi$;

$I_{vT\rho C_p}$, $= \int_{-1}^{1} f_v f_T f_\rho f_{C_p} \,d\xi$;

$I_{vv\rho}$, $= \int_{-1}^{1} f_v^2 f_\rho \,d\xi$;

$I_{v\rho}$, $= \int_{-1}^{1} f_v f_\rho \,d\xi$;

I_ρ, $= \int_{-1}^{1} f_\rho \,d\xi$;

* Present address: Technion—Israel Institute of Technology, Haifa, Israel.

† Present address: Cummins Engine Co., Columbus, Indiana, U.S.A.

k, heat conductivity;
k_D, a constant for the prediction of C_d given in [11];
m, mass;
$\dot{m}_L$, mass flux of the liquid through the nozzle orifice;
Nu, Nusselt number for heat transfer;
N'_u, Nusselt number for mass transfer;
Pr, $\bar{C}_p\bar{\mu}/\bar{k}$, Prandtl number;
p, pressure;
p_{Ls}, partial pressure of the vapour on the surface of the droplet;
P_T, total pressure in a gaseous mixture (not static plus dynamic pressure);
R, transformed θ co-ordinate;
R', $= \mathrm{d}R/\mathrm{d}\Theta$;
R'', $= \mathrm{d}^2R/\mathrm{d}\Theta^2$;
Re, $= d_{sa}v_r\bar{\rho}/\bar{\mu}$, Reynolds number;
R'_e, $= d_{sa}v_r\rho_g/\mu_g$;
R_g, gas constant of the gas;
R_v, gas constant of the vapour;
r, radius of the polar co-ordinate system (Fig. 1);
r', $= \mathrm{d}r/\mathrm{d}\theta$;
r'', $= \mathrm{d}^2r/\mathrm{d}\theta^2$;
r_a, external radius of the swirl;
Sc, $\bar{\mu}/\bar{\rho}D$, Schmidt number;
T_d, temperature of the mean drop;
T_{eq}, equivalent temperature defined in equation (12);
T_{ev}, evaporation temperature of the liquid;
ΔT, $= T - T_{eq}$;
t, time;
u, tangential velocity of the swirl;
u_{eq}, equivalent velocity of the swirl, defined in equation (11);
v, velocity inside the spray in the direction of the centre line;
v_r, relative velocity of a drop;
Δv, $= v - u_{eq}$;
x, co-ordinate along the centre line (Fig. 1);
y, co-ordinate perpendicular to x;
z, $= \dfrac{(\mathrm{d}m/\mathrm{d}t)\,C_L}{hA}$;
α, $= u_{eq}/v_{mo}$;
β, angle between centre line and the tangential direction (Fig. 1);
Θ, transformed θ co-ordinate;
θ, angle in the polar co-ordinate system (Fig. 1);
$\hat{\Theta}$, $= T_{mo}/T_{eq}$;
κ, evaporation function defined in equation (1);
μ, dynamic viscosity;
ξ, $= y/b$, normalized co-ordinate perpendicular to the centre line;
ρ, density of the mixture defined in equation (14);
ρ_s, $= (\rho_{mo}/2)\,I_\rho$, mean density of the spray (function of x);
ϕ, functions of the spray quantities defined ahead of equation (13);
ψ, $= (1 - c_{mo}\phi_c\kappa)\left[\dfrac{1 - \phi_c c_{mo}}{1 - \phi_c c_{mo}\kappa} + \dfrac{\phi_c c_{mo}(1-\kappa)}{(1 - \phi_c c_{mo}\kappa)}\dfrac{R_v}{R_g}\right]$, a function in equation (17).

Subscripts

c, of the concentration;
g, of the gas;
L, of the liquid;
m, on the centre line;
o, at the initial cross section;
T, of the temperature;
v, of the velocity.

Superscripts

0, at the initial cross section;
~, vectorial quantity;
–, algebraic average between value for gas and value for vapour.

INTRODUCTION

THE INJECTION of a liquid spray into a flow field of hot gases is utilized in many branches of modern technology such as Diesel Engines, Otto Engines with fuel injection, Jet Engines, Gas Turbines, Burners, Air Conditioners, Water

Desalination and many chemical production processes. It is, therefore, not surprising that the mixing of a liquid spray in hot gases is not a new subject for research.

One way of approach is based on the calculation of the histories of single drops vaporizing in a gas stream as described by El Wakil [1] and later by Eisfield [2] and Borman and Johnson [3]. Once the histories of single drops of various diameters are calculated, the desired information on the mixing region can be obtained by superposition of the particular histories based on a known size distribution of the drops at the initial cross section of the spray. The accuracy of this approach is questionable as the interaction between the drops in the spray cannot properly be accounted for in this mathematical model.

Dlauhy and Gauvin [4] and Bosé and Pei [5] tried to correct this deficiency by using the Sauter mean diameter in the correlations of the Nusselt numbers for heat and mass transfer originally developed by Ranz and Marshall [6] for single drops. Their results are confirmed experimentally but their work is confined to straight sprays in parallel flow, thus imposing a serious restriction on its application.

A more general approach based on continuum mechanics was developed by Wakuri *et al.* [7] and Catton *et al.* [8]. Their works are limited to the calculation of the spray penetration only, thus restricting the scope of the information obtainable.

This paper presents a new, more comprehensive method to yield not only penetration and mixing region geometry, but also approximate velocity, concentration and temperature fields as well as the rate of evaporation. The method, being based on continuum mechanics and using the Sauter mean diameter in the evaporation model, is capable of taking the interaction between the drops within the spray into consideration. The present model is developed for sprays injected into swirling gas. However, due to its general character, it can easily be applied to injections into arbitrary flow fields with minor modifications only.

The present paper deals only with the first phase of this new approach, and much remains yet to be done.

THE PHYSICAL MODEL AND ITS MATHEMATICAL FORMULATION

The development of the present method followed two decisions. Firstly it was clear that a theory being able to take proper account of the interaction between the droplets within the spray must not be based on the single droplet theory. Secondly, it was realized that a treatment on the basis of continuum mechanics is required applying the equations of continuity, momentum, energy and diffusion. This necessitates the introduction of a differential volume element (much larger in size than each individual droplet) in the mixing zone having an equivalent mass of the total mass of gas, liquid droplets and evaporated liquid contained in the element. The element is, therefore, characterised completely by its concentration and an "evaporation function" defined as the ratio between the mass of the yet unevaporated droplets to the total mass of the injected matter (liquid plus vapour) contained in that element [see equation (1)]. Equations of continuity, diffusion, energy, momentum, state and evaporation can then be written to solve for concentration, velocity, pressure, temperature, density and "evaporation function" as functions of space. As turbulent mixing is to be considered, these equations with the exception of evaporation, must be in the time-mean form incorporating terms for heat and mass transfer similar to the Reynolds stresses in the turbulent viscous flow study. Very little is known about turbulent momentum, mass and heat-transfer coefficients required for the solution. Furthermore, inquiry into the more simple cases of incompressible and isothermal flow of simple geometry already showed the immense stability and convergence difficulty in the numerical solution of problems of this type which must be applied due to the complexity of the equations involved. It was, therefore, decided that at this stage of our knowledge, it would be more profitable not to

look at the problem so closely and in such detail using the partial differential formulation, but to step backwards and look at it in a more macroscopic or coarser term. A simpler physical model will have to be constructed which would lend itself to mathematical analysis. The treatment naturally would be less rigorous but it is hoped that the salient features of the true physical process would be revealed.

Because of the similarity of the boundary-layer flow and jet or spray flow, the established techniques in solving boundary-layer problems can be used to describe the detailed structure of the spray based on its centre line. Thus, by assuming similarity profiles for the velocity, concentration and temperature distribution inside the spray, the powerful integral method can be used, which transforms the partial differential equations into a set of ordinary differential equations with the distance along the spray centre line as the independent variable. There needs to be no restriction on the exact nature of the profiles so long as the boundary conditions at the edges of the spray are satisfied.

The geometry of the mixing region is given in Fig. 1, which also describes the main parameters as well as the co-ordinate systems used in the mathematical model. The external flow field is considered to be two dimensional and steady. The spray has a circular origin, its horse shoe shaped cross-sections [9] are approximated by rectangular cross-sections of constant height to width ratio. In this way, a quasi two dimensional formulation, is obtained. The fact that the phenomenon is considered to be steady leads to a physical model which is somewhat artificial in the sense that a continuous line sink and behind it a continuous line source must be located on two radii as close to the origin of the spray as desired without affecting the source of the spray.

The mathematical model consists of three main parts allowing the calculation of the evaporation function, the spray analysis and the centre line. The results of each part are used as known functions in the solution of the subsequent part. The calculation of the evaporation function requires the shape of the centre line which is not yet known at the start of the solution, thus an iterative procedure is required for the solution.

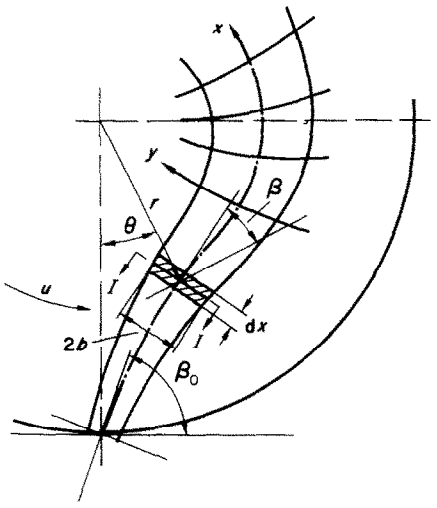

FIG. 1. The geometry of the spray.

1. *The evaporation function*

Using the theory of El Wakil *et al.* [1] with the correlations of Bosé and Pei [5] instead of those of Ranz and Marshall [6], originally used by El Wakil, an evaporation function for the spray can be calculated. This evaporation function, κ, is defined as the ratio between the mass of the yet unevaporated liquid at an arbitrary downstream position to the total mass of injected liquid (being the sum of yet unevaporated liquid, plus vapour) expressed in terms of Sauter mean diameters

$$\kappa = \frac{m}{m_o} = \left(\frac{d_{sa}}{d_{sao}}\right)^3. \tag{1}$$

Being the ratio between two mean quantities of the spray, the evaporation function is a non-dimensional function of the distance along the centre line of the spray, x, describing the mean

state of vaporization of the spray. The following three equations which are a modified version of the equations originally derived by El Wakil *et al.* [1], enable the calculation of the history of a mean drop yielding the value of the mass of the liquid droplets, m, required for the calculation of the evaporation function.

From mass transfer considerations we have:

$$\frac{dm}{dt} = -\frac{\pi d_{sa}\bar{D}p_T}{\bar{p}_g/\bar{\rho}} \ln\left[\frac{p_T}{p_T - p}\right] Nu'. \quad (2)$$

From heat transfer considerations

$$\frac{dT_d}{dt} = \frac{\pi k d_{sa}(T_g - T_d)}{mC_L} \frac{z}{e^z - 1} Nu + \frac{H}{mC_L}\frac{dm}{dt}. \quad (3)$$

From drop dynamics considerations

$$\frac{dv_r}{dt} = -\tfrac{9}{2} C_d \frac{\rho_g}{\rho_L} \frac{v_r^2}{d_{sa}}. \quad (4)$$

The drag coefficient in equation (4) is calculated with Ingebo's correlation [11]. It can be questioned whether this is the best choice. However, no data relating to evaporating drops in sprays are available at present. As long as this gap in our knowledge is not closed one is forced to rely on single droplet data, introducing the Sauter mean diameter into the calculation of the drag coefficient. No other single droplet based method for the prediction of the drag coefficient is more justified at these conditions.

The Nusselt numbers in these equations are given by the correlations of Bosé and Pei [5] which are based on spray experiments rather than single droplet experiments.

$$Nu = 2 + 0{\cdot}6\, Pr^{\frac{1}{3}}\, Re^{\frac{1}{2}} \quad (5)$$

$$Nu = 2 + 0{\cdot}6\, Sc^{\frac{1}{3}}\, Re^{\frac{1}{2}}. \quad (6)$$

The dimensionless numbers in these correlations are defined as follows:

$$Pr = \frac{\bar{C}_p\bar{\mu}}{\bar{k}} \quad (7)$$

$$Re = \frac{d_{sa}\, v_r \bar{\rho}}{\bar{\mu}} \quad (8)$$

$$Sc = \frac{\bar{\mu}}{\bar{\rho}\bar{D}}. \quad (9)$$

The mean film properties are assumed constant according to their definition but v_r and d_{sa} of the Reynolds number are variables of the problem. Thus, equations (2)–(4) are coupled and must be solved simultaneously.

The source of the spray is the common geometrical point at which the three differential equations have their boundary conditions at an arbitrary moment $t = 0$. (The moment at which the boundary conditions are specified is arbitrary as the phenomenon is steady, while the time serves as parameter in this formulation, chosen because of convenience in the description of the history of a drop as it travels through the mixing region.)

The solution of equation (2)–(4) yields three functions of time, namely: $m(t)$; $T_d(t)$ and $v_r(t)$. These functions are transformed into functions of x through the equation connecting time and distance travelled

$$x = \int_0^t |(\tilde{u} + \tilde{v}_r)|\, dt. \quad (10)$$

The vectorial sum $\tilde{u} + \tilde{v}_r$ gives the mean absolute velocity of the drops in the spray. As nothing is known about the direction of the relative velocity, the summation must be carried out knowing the shape of the centre line of the spray, the direction of which is identical with the direction of the mean absolute velocity of the drops. This shape is not *a priori* known being a result of the third part of the mathematical model. Thus, an iterative procedure is required, where the centre line in the first approximation is assumed.

2. *The spray analysis*

The second main part of this formulation, the spray analysis, yields the approximate fields of the velocity, temperature and concentration inside the mixing region. Further it gives the width of the mixing region. It is based on the integral conservation conditions of momentum,

heat content and injected matter inside the mixing region. The procedure is similar to the integral methods of boundary layers along curved walls. Because of the turbulent nature of the flow, the momentum, temperature and concentration profiles across the spray can be assumed to have the same width. The solution is carried out in an orthogonal co-ordinate system in which the not yet known centre line is the axis of zero ordinate (Fig. 1).

Two average quantities are introduced to simplify the formulation. The equivalent velocity, u_{eq} and the equivalent temperature T_{eq}. u_{eq} is the ratio between the momentum flux and the mass flux of the undisturbed flow field prior to start of the injection

$$u_{eq} = \int_0^{r_a} \rho u^2 \, dr / \int_0^{r_a} \rho u \, dr. \tag{11}$$

The equivalent temperature is a measure of the average temperature in the flow field during the mixing process. It is defined as the equilibrium temperature of an imaginary process in which half of the injected liquid flux is heated up by the gas stream to its evaporation temperature, evaporated and then superheated to the temperature, T_{eq}.

$$T_{eq} = \frac{C_{pg} T_g \int_0^{r_a} \rho_g u \, dr - \frac{1}{2}\dot{m}_L [(T_{ev} - T_L) C_L + H + T_{ev} C_{pv}]}{C_{pg} \int_0^{r_a} \rho_g u \, dr - \frac{1}{2}\dot{m}_L C_{pv}}. \tag{12}$$

The spray analysis is not solved in terms of absolute velocity and temperature. Instead a velocity difference $\Delta v = v - u_{eq}$ and a temperature difference $\Delta T = T - T_{eq}$ are introduced. The concentration is not altered and absolute values are used as the outside concentration is zero. Universal similarity profiles of the velocity, $\Delta v/\Delta v_m = f_v(\xi)$, the temperature $\Delta T/\Delta T_m = f_T(\xi)$ and the concentration $c/c_m = f_c(\xi)$ are used to allow a convenient formulation of the integral method. The actual distribution of these quantities can be obtained through Δv_m, ΔT_m, c_m and b at any point along the centre line of the spray. It must be pointed out that the real profiles in a spray deflected by a lateral flow are not similar. The similarity assumption was introduced here as first approximation. More accuracte profiles can be used by introducing three or four parameter profiles, rather than the two parameter profiles used here. This required also the addition of more conservation conditions to the mathematical formulation. The parameters of the similar profiles which are the unknowns of the spray analysis are replaced for convenience by dimensionless quantities $\phi_v(x) = \Delta v_m/\Delta v_{mo}$; $\phi_T(x) = \Delta T_m/\Delta T_{mo}$; $\phi_c(x) = c_m/c_{mo}$ the width b is not altered. Like the parameters, these dimensionless quantities are functions of x only.

Four equations are required for a solution. The condition of integral conservation of momentum gives:

$$\phi_v = -\frac{I_{v\rho}\alpha}{2 I_{vv\rho}(1-\alpha)} + \left[\left(\frac{I_{v\rho}\alpha}{2 I_{vv\rho}(1-\alpha)}\right)^2 + \frac{b_o^2 [I^o_{vv\rho} + (\alpha/1-\alpha) I^o_{v\rho}]}{b^2 I_{vv\rho}}\right]^{\frac{1}{2}}. \tag{13}$$

The integrals, I, defined in the nomenclature, are a function of x as they contain the term $f_\rho = \rho/\rho_0$. The density, ρ, is a function of both x and the co-ordinate perpendicular to it, it is an additional unknown of the problem but can be expressed with the help of the equation of state, in terms of the other unknowns.

$$\rho = \left\{ \frac{(1 - f_c\phi_c c_{mo}\kappa)\left[\dfrac{1 - f_c\phi_c c_{mo}}{1 - f_c\phi_c c_{mo}\kappa} R_g + \dfrac{f_c\phi_c c_{mo}(1-\kappa)}{1 - f_c\phi_c c_{mo}\kappa} R_v\right]}{p} (T_{eq} + f_T\phi_T\Delta T_{mo}) + \frac{f_c\phi_c c_{mo}\kappa}{\rho_L} \right\}^{-1} \tag{14}$$

The evaporation function, κ, in equation (14) is known at this stage, being a result of the first part of the mathematical model.

The integral conservation of the injected matter gives:

$$\phi_c = \frac{(b_o/b)^2\,[I^o_{vc\rho} + (\alpha/1-\alpha)\,I^o_{c\rho}]}{\rho_v I_{vc\rho} + (\alpha/1-\alpha)\,I_{c\rho}} \tag{15}$$

The fourth equation of the spray analysis describes the growth of the mixing region. The argument is based on Prandtl's mixing length theory, and the development of the equation follows that of Abramovich ([9], p. 268), modified to cover the present, rather more complicated phenomenon.

$$\frac{db}{dx} = c_b\left[\frac{2}{1 + [\phi_T(\hat{\Theta} - 1) + 1]\,\psi + pc_{mo}\phi_c\kappa/(R_g T_{eq}\rho_L)} + 2\frac{\alpha}{(1-\alpha)\phi_v}\frac{1}{1}\right]^{-1}. \tag{17}$$

where the integrals I are again defined in the nomenclature. The integral conservation of heat content for the two phase evaporating spray yields:

$$\begin{aligned}\phi_T = \Bigg\{\left(\frac{b_o}{b}\right)^2 \Bigg[& \frac{c_{T1}\rho_{mo}}{\Delta T_{mo} c_{mo}} I^o_{v\rho} + \frac{c_{T1}\rho_{mo}}{\Delta T_{mo} c_{mo}}\frac{\alpha}{1-\alpha} I^o_{\rho} \\ & + \frac{c_L\rho_{mo}}{c_{mo}} I^o_{vT\rho Cp} + \frac{c_L\rho_{mo}}{c_{mo}}\frac{\alpha}{1-\alpha} I^o_{T\rho Cp}\Bigg] \\ & - \Bigg[c_{T2}(\kappa C_L + (1-\kappa)C_{pv} - C_{pg})\,\phi_v\phi_c I_{vc\rho} \\ & + c_{T2}(\kappa C_L + (1-\kappa)C_{pv} - C_{pg})\frac{\alpha}{1-\alpha}\phi_c I_{c\rho} \\ & + H\frac{\rho_{mo}}{\Delta T_{mo}}(1-\kappa)\,\phi_v\,\phi_c\,I_{vc\rho} \\ & + H\frac{\rho_{mo}}{\Delta T_{mo}}\frac{\alpha}{1-\alpha}(1-\kappa)\,\phi_c\,I_{c\rho}\Bigg]\Bigg\} \\ & \times \left[\frac{C_L\rho_{mo}}{c_{mo}}\phi_v I_{vT\rho Cp} + \frac{C_L\rho_{mo}}{c_{mo}}\frac{\alpha}{1-\alpha} I_{T\rho Cp}\right]^{-1}. \end{aligned} \tag{16}$$

$\hat{\Theta}$ and ψ are defined in the nomenclature. A universal value of the coefficient c_b can be assumed as first approximation to cover also the case of an evaporating spray ([9], pp. 190, 315, 330, 550, 588). The accuracy of this assumption requires additional investigation.

3. *The centre line calculation*

The four simultaneous equations (13), (15)–(17) yield the approximate mixing field in terms of the four parameters Δv_m, ΔT_m, c_m and b of the assumed profiles in the mixing region. This mixing field is based on the centre line on which ξ is zero. This centre line is not yet known, it can be calculated at this stage using the results of the spray analysis. The resulting centre line may be used for a more accurate calculation of the evaporation functions with which a new cycle of calculations may be started. This can be repeated until a satisfactory degree of convergence is reached.

The calculation of the centre line is based on

the dynamic equilibrium of a spray segment, dx, (Fig. 1) which is considered for this purpose to be quasi solid. The forces acting on this segment in a deflecting flow are the gas force and the centrifugal force due to the curvature of the path along which the segment is moving. Thus the condition of equilibrium is:

$$dF_g \pm dF_c = 0. \tag{18}$$

Here, outward acting forces are given a positive sign. Thus, the sign of the centrifugal term depends on the curvature of the centre line.

Equation (18) is developed into a convenient form in terms of the polar co-ordinate system of Fig. 1.

$$r'' = r + 2\frac{r'^2}{r} \pm \frac{(r^2 + r'^2)^{\frac{3}{2}}}{r} \left[C_{de} \left(\frac{\rho_g}{\rho_s}\right) \left(\frac{u}{v_m}\right)^2 \frac{\sin^2 \beta}{4b} \right]. \tag{19}$$

This is the differential equation of the centre line. The angle β (Fig. 1) is given through:

$$\beta = \tan^{-1}(r/r') - \frac{\pi}{2}. \tag{20}$$

ρ_s is a mean density of the spray defined in the nomenclature. It is a result of the spray analysis, as are also the quantities v_m and b. The deflection coefficient C_{de} represents the gas forces acting on the spray. Not much is known at present about its value (see section dealing with preliminary experimental results). Experiments are now under way designed to establish a reliable correlation for the prediction of this deflection coefficient.

SOLUTION OF THE EQUATIONS

Due to the complexity of the mathematical formulation, an analytical solution is not possible at the present state of art. Thus, a numerical procedure for the solution of the equations and an appropriate computer program were developed to yield the calculated results presented here.

The nature of the boundary conditions of the evaporation function equations suggests a forward integration method to be applied. A fourth order Runge–Kutta method proved to be satisfactory. Not much is known about the calculation of Sauter mean diameter required as input data. A number of authors published empirical correlation to suit their particular experiments but no general method is known at present. This is not surprising because the droplet size distribution in a spray is strongly affected not only by physical quantities such as properties of liquid and gas, pressures and velocities, but also by the geometry of the nozzle used to produce the spray. Thus, information on the atomization characteristic of the particular nozzle used, must be known if assumptions on the initial droplet diameter are to be avoided. In the present investigation, diesel injectors were used to produce the spray. Therefore, the Sauter mean diameter is calculated with a formula given by Knight (10). This empirical formula is developed for swirl atomizers, but can also be used satisfactorily in diesel sprays according to Knight's observations, communicated privately. The values of the saturation pressure of the liquid for the varying drop temperature, T_d, required during the computation are computed during the solution with a polynomial of the tenth degree in T_d. The coefficients of the polynomial are calculated from known physical data of the liquid in question. The values of the droplet drag coefficient, C_d, are taken from Ingebo's study [11].

Like the evaporation function, the four interdependent spray analysis equations have their boundary conditions given at a common point, i.e. the source of the spray. It is, therefore, again convenient to use the fourth order Runge–Kutta method. Three of the equations in question are integral equations while the equation of the spray width growth is differential. Properly, the time consuming integrations to be performed in the integral equations (which are carried out by a ten point Gaussian quadrature) should be incorporated in the Runge–Kutta procedure.

This causes the seven integrations involved to be carried out four times in every integration step of the differential equation. Considerations of computation economy lead to a simpler but less accurate numerical procedure where the integral equations are solved outside the Runge–Kutta procedure using the spray width, b, of the previous step. The resulting values of ϕ_v, ϕ_T and ϕ_c are then substituted as constants into the Runge–Kutta step calculating the new value of b. The error involved in this simplified procedure is a function of the step length and the data. Thus, for each set of data such a step length must be chosen that the error would be kept within reasonable bounds. The values of the evaporation function required are computed during the solution of the spray analysis through a polynomial of the tenth degree in x. The coefficients of this polynomial are calculated from the previously calculated evaporation function.

The numerical solution of the centreline equation is carried out in the r, θ co-ordinate system of Fig. 1 again with a fourth order Runge–Kutta method. For this purpose, the second order equation is transformed into two simultaneous first order differential equations. The values of ρ_s, v_m and b required for the solution are calculated during the computation through tenth order polynomials in x. The coefficients of these polynomials are calculated from the results of the spray analysis. The value of x required to determine ρ_s, v_m and b is calculated in every integration step. The value of u is determined through a tenth order polynomial in r representing the known undisturbed velocity distribution in the swirl.

The path of a spray injected in radial direction or a spray injected against the direction of the swirl includes a point at which $\mathrm{d}r/\mathrm{d}\theta \to \infty$. At this point and in its neighborhood, the numerical integration can not be carried out. To overcome this difficulty, the integration of the centre line equation in this region is carried out in a cartesian R, Θ co-ordinate system which is rotated by $\pi/2$ anticlockwise relative to a cartesian, r, θ co-ordinate system in which r and θ have their numerical values of the polar system, measured along the cartesian axes. The differential centre line equation has no physical meaning in these two systems which serve only for the transformation necessary to overcome the difficulty involved in the presence of a singular point in the interval of integration. The centre line equation in the R, Θ system has the following form:

$$R'' = -\Theta(R')^3 - 2\frac{R'}{\Theta} \pm \frac{[\Theta^2 (R')^2 + 1]^{\frac{3}{2}}}{\Theta} \times \left[C_{de} \left(\frac{\rho_g}{\rho_s}\right) \left(\frac{u}{v_m}\right)^2 \frac{\sin^2 \beta}{4b} \right]. \quad (21)$$

Where

$$\beta = \tan^{-1}(-\Theta R') - \pi/2. \quad (22)$$

At a point at which $\mathrm{d}r/\mathrm{d}\theta \to \infty$ we have $\mathrm{d}R/\mathrm{d}\Theta \to 0$ so that the integration in the R, Θ system is straight forward at this point. The computer program of the centre line integration includes a routine which senses the approach to a singular point and which automatically transformes the r, θ co-ordinate system and the equation into the R, Θ plane. Once the integration passed the singular point, a transformation back into the r, θ system is carried out.

SOME RESULTS OF INITIAL CALCULATIONS

As the computer programs were developed for each of the three sections of the mathematical model, opportunity was taken to carry out calculations with systematical variation of the various parameters involved.

The object of these calculations was not only to confirm qualitatively the correctness of the model, but also to have a feel of the relative importance of various parameters examined. The calculations were performed for acetone or Freon injected into helium or nitrogen. A basic set of data was used of which the single parameter examined was varied.

Figure 2 shows the variation of the evaporation function due to variations in the parameters indicated. Other basic input data are given in

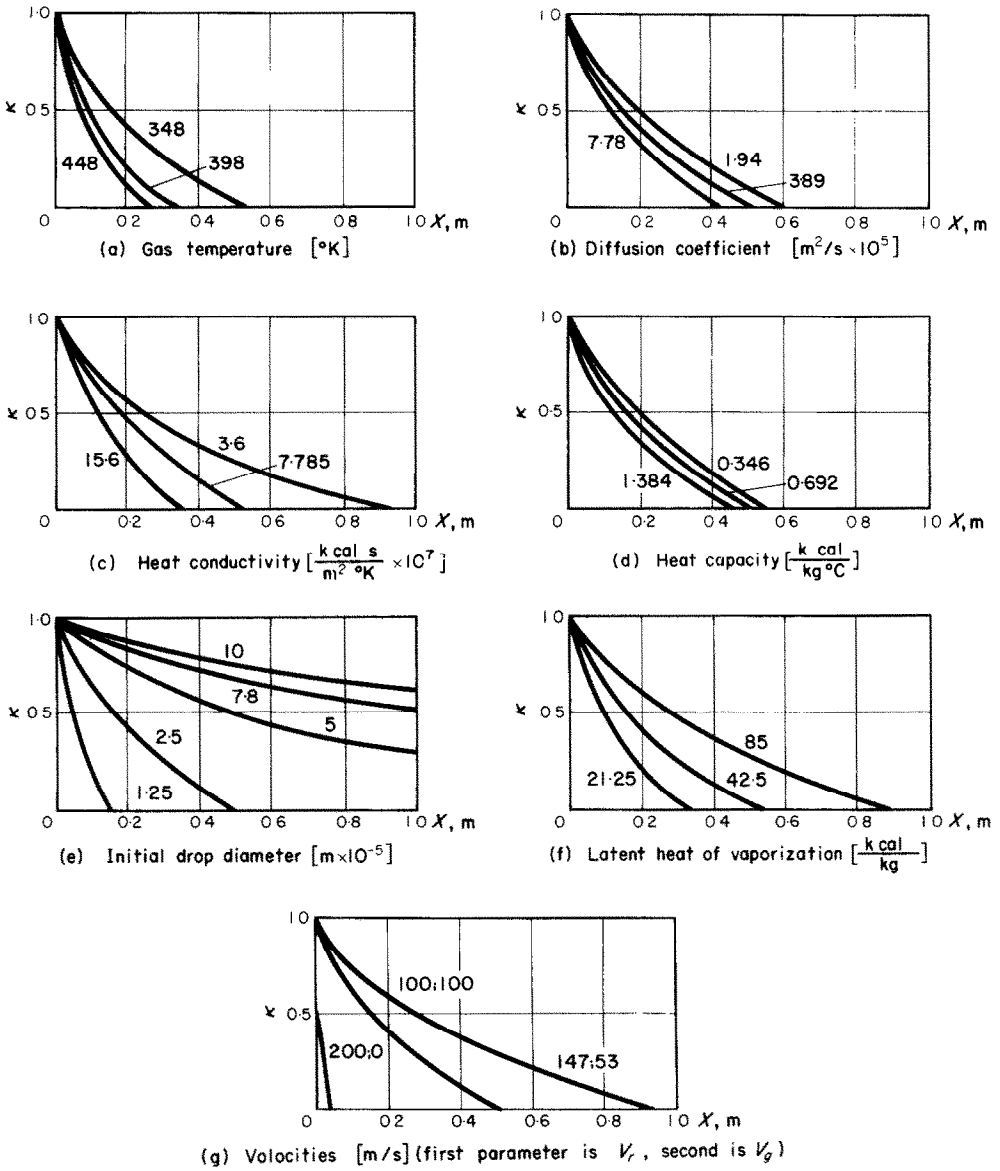

FIG. 2. The effect of various parameters on the evaporation function.

Appendix 1. The figures show an increase in the evaporation rate due to higher gas temperatures (Fig. 2a), larger diffusion coefficients of the system (Fig. 2b), larger heat conductivity of the film around the drop (Fig. 2c), and larger heat capacity of that film (Fig. 2d). Larger initial drop diameters (Fig. 2e) and larger latent heat of vaporization (Fig. 2f), on the other hand, result in decreased rates of evaporation. Figure 2g, shows the effect of variations in the velocities.

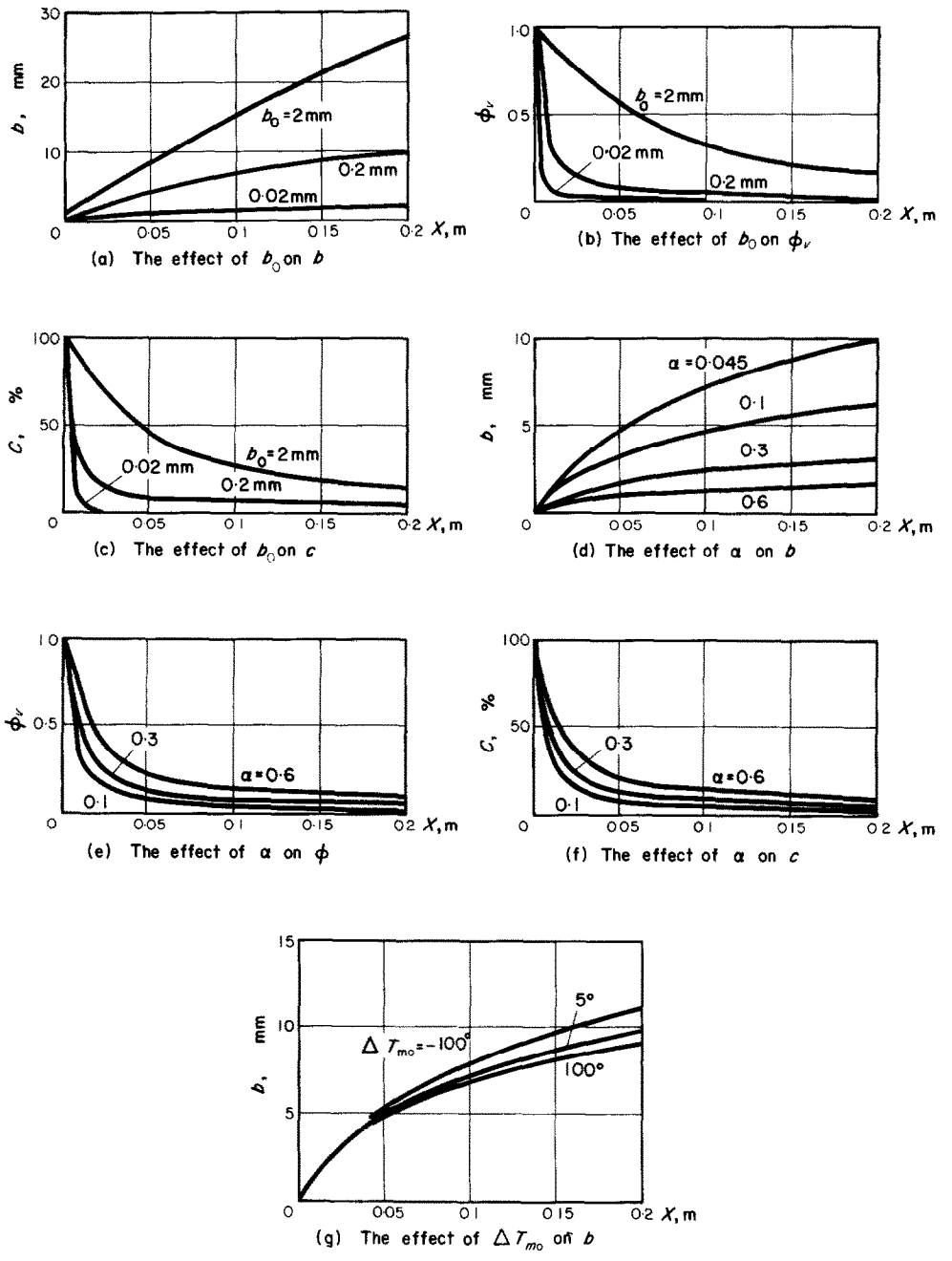

FIG. 3. Effects of the initial spray width, b_o, velocity ratio, α, and initial temperature differences, ΔT_{mo}, on the development of the mixing region.

The comparison is done for sprays of constant initial velocity of 200 m/s. The change in the evaporation function is due to the combined effect of the relative velocity on the evaporation rate of the drop and the transport effect of the gas flow which carries the drop in a downstream direction.

The results of the spray analysis study are given in Fig. 3. Its basic set of data is also given in Appendix 1. The similarity profiles used are those given by Abramovich [9] namely:

$$f_v(\xi) = (1 - \xi^{\frac{3}{2}})^2, \qquad f_T(\xi) = 1 - \xi^{\frac{3}{2}},$$
$$f_c(\xi) = 1 - \xi^{\frac{3}{2}}.$$

As can be seen from Figs. 3a–3c, a larger initial spray cross section results in a wider and stronger spray as would be anticipated. The effect of an increase in the initial velocity ratio is summarized in Figs. 3d–3f. Figure 3g shows the influence of the initial temperature difference on the growth of the spray, confirming the well known fact that cooled jets spread less than heated jets.

The study of the centre line equation is carried out with basic data given in Appendix 1. Figure 4a shows the effects of variations in the injection angle for inward injection. Figure 4b shows the same effect for outward injections. The influence of the initial velocity ratio is given in Figs. 4c and 4d again for inward and outward injections. The effect of the evaporation rate in the spray on the shape of the centre line is given in Fig. 4e. It can be seen that the resistance of the spray to the deflecting flow is reduced the larger the rate of evaporation.

PRELIMINARY EXPERIMENTAL RESULTS

The results of the above analysis must be confirmed experimentally and in particular values of the deflection coefficient C_{de} must be established. Experiments are now under way which are intended to supply the necessary information. At present a limited amount of experimental results obtained by the authors is available. In addition, a number of experiments carried out at C.A.V. Ltd., Acton, England, were used. These experiments were carried out by a method described in [12]. The data of all these experiments are summarized in Table 1.

In the experiments carried out by the authors an acetone spray from a diesel injection system modified to deliver a single injection only, was injected into a number of nitrogen swirls of known velocity distribution. The two dimensional swirl was created by releasing nitrogen from a pressurized vessel through a tangential slot into a cylindrical swirl chamber. The decay period of the swirl in all experiments (including those of C.A.V.) is long enough compared to period of injection so that a steady gas flow during the mixing period can be assumed. Further, the characteristic of the injection in all experiments was close to a step function due to appropriate shape of the injector needle. Thus, the mixing process can be regarded approximately steady after the start of the injection. In the acetone injection, the spray was photographed towards the end of the injection (Figs. 5a–5c). The spray of the C.A.V. experiments was recorded with a cinematographic technique [12]. Single frames of the resulting film were used in the present investigation (Figs. 6a–6c). The photographic records are compared with mixing regions calculated along the lines described here (Figs. 7 and 8).

In the calculation of the centre lines, the newly defined deflection coefficient is used which was never before utilized in calculations of this type so that nothing is known about its evaluation. Therefore, the centre line calculations were repeated with various values of C_{de}. The appropriate deflection coefficient was chosen to fit best the experimental observations. Each of the figures consists of two parts:

(a) shows the different centre lines for a particular injection calculated with
(a) various values of the deflection coefficient, and

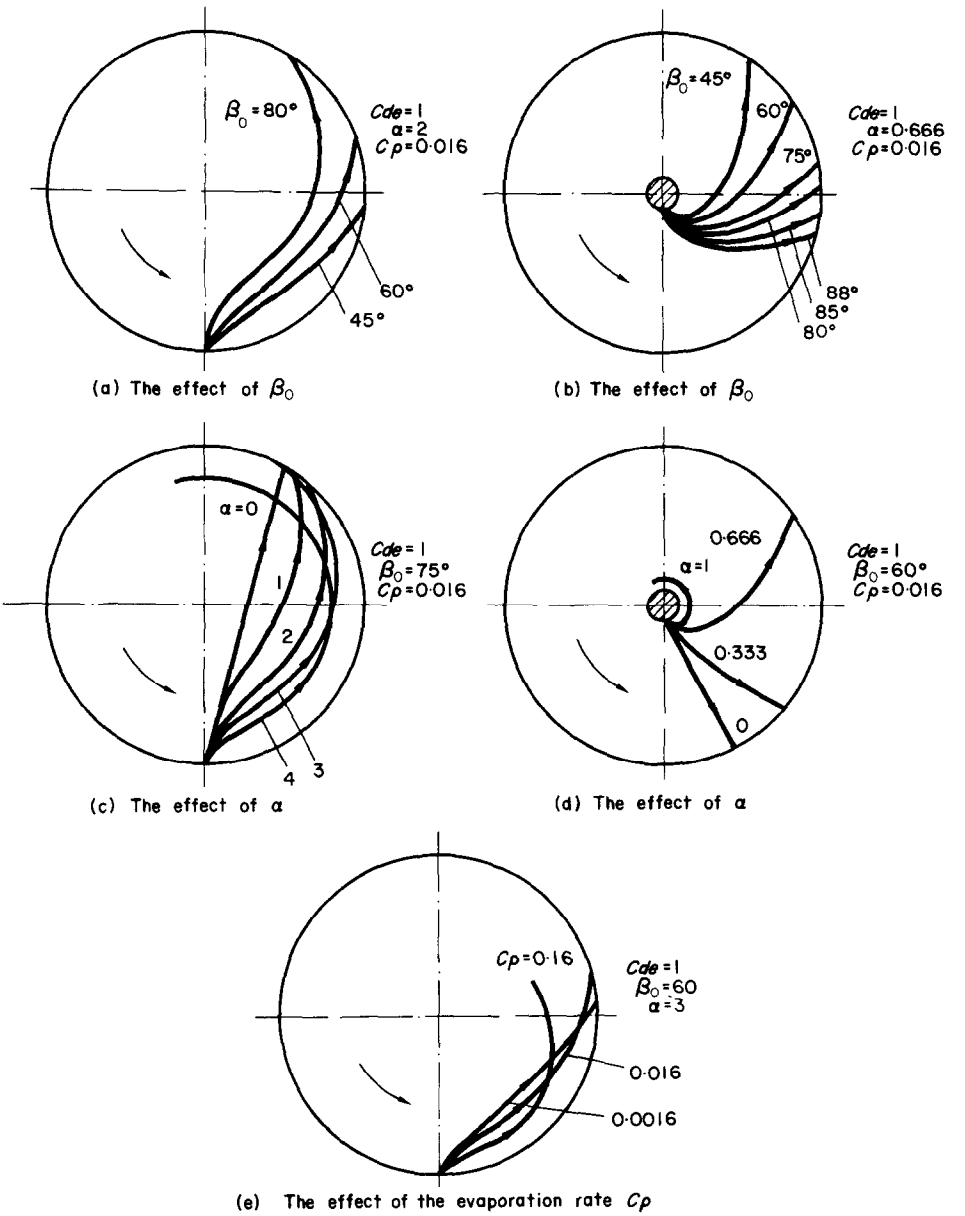

FIG. 4. The effect of some basic parameters on the development of the centre line.

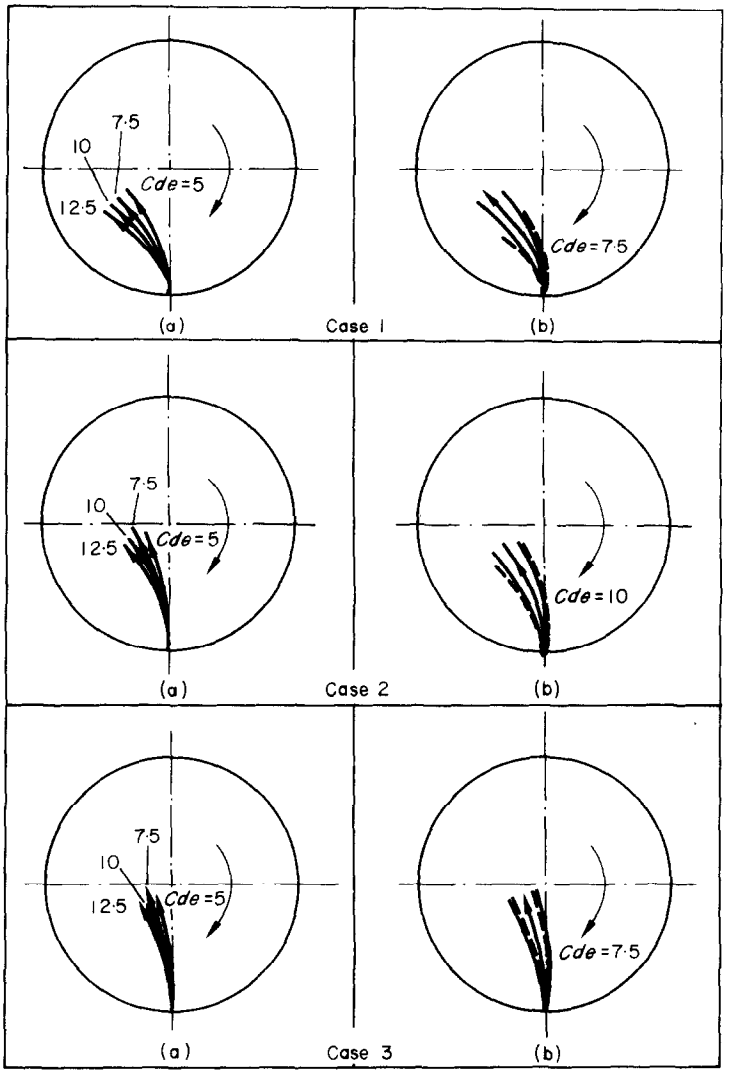

FIG. 7. Calculated and photographed mixing regions of acetone injections (centre lines on the left are calculated with C_{de} variation, the figures on the right compare the best fitting calculation to the photographed contour given in dashed lines).

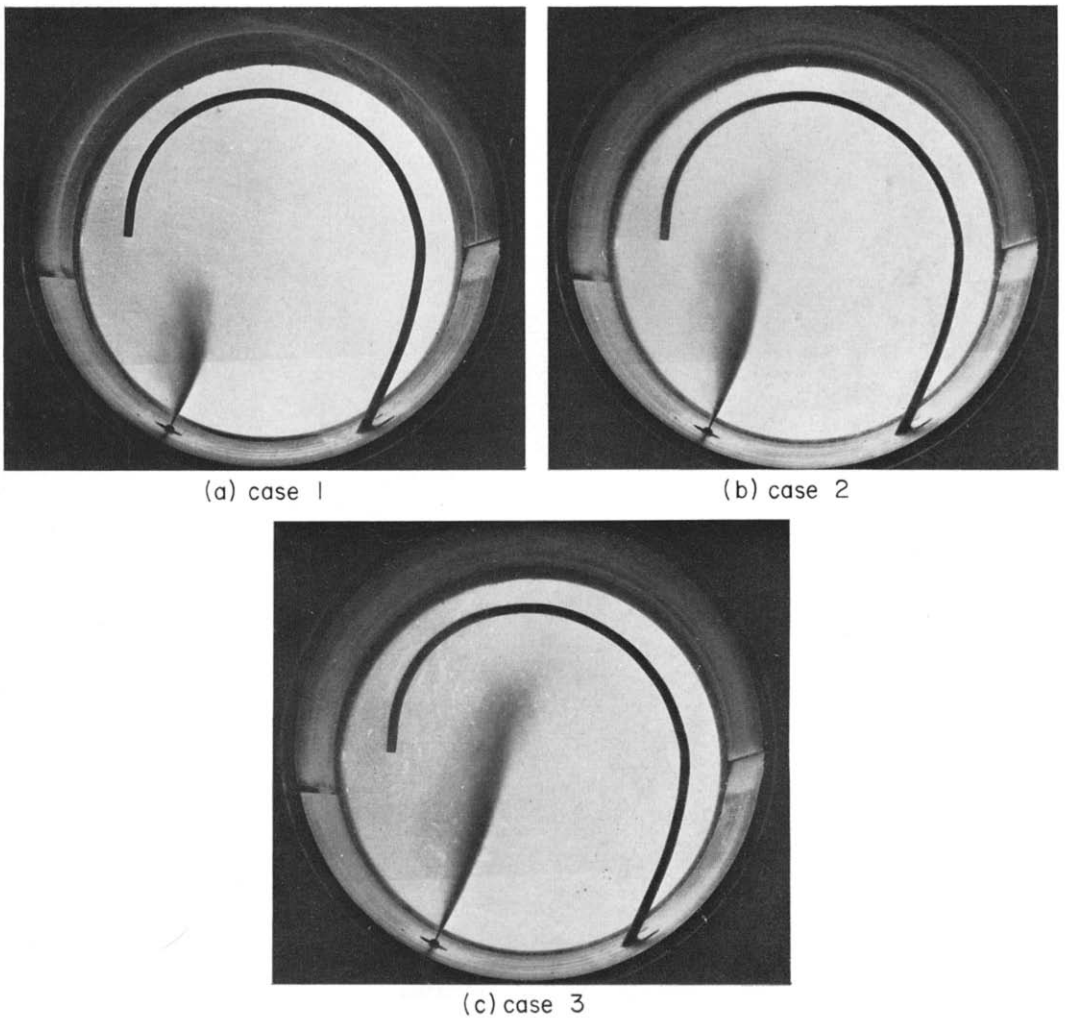

FIG. 5. Photographed mixing regions of cases 1–3.

[*facing page 806*

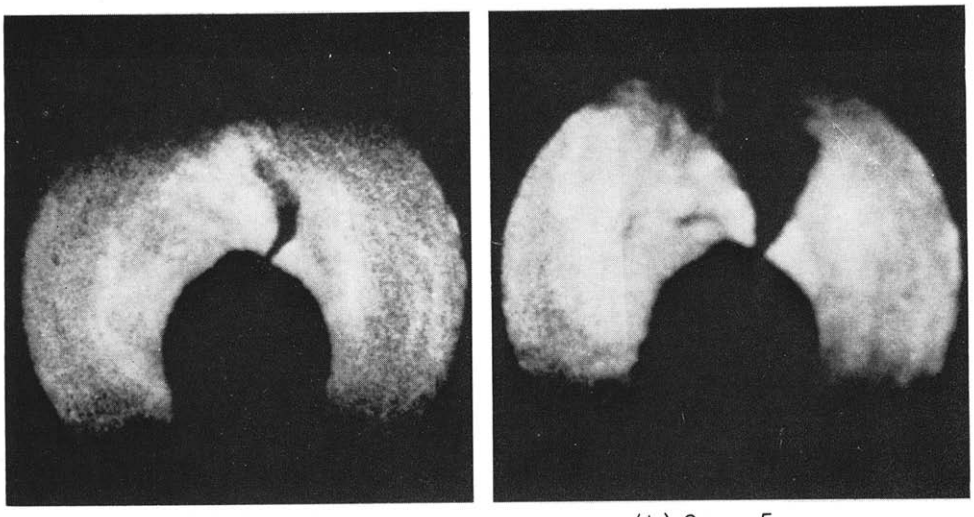

(a) Case 4 (b) Case 5

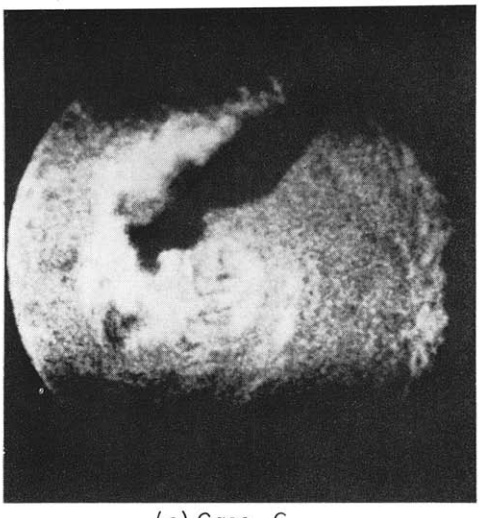

(c) Case 6

FIG. 6. Photographed mixing regions of cases 4–6.

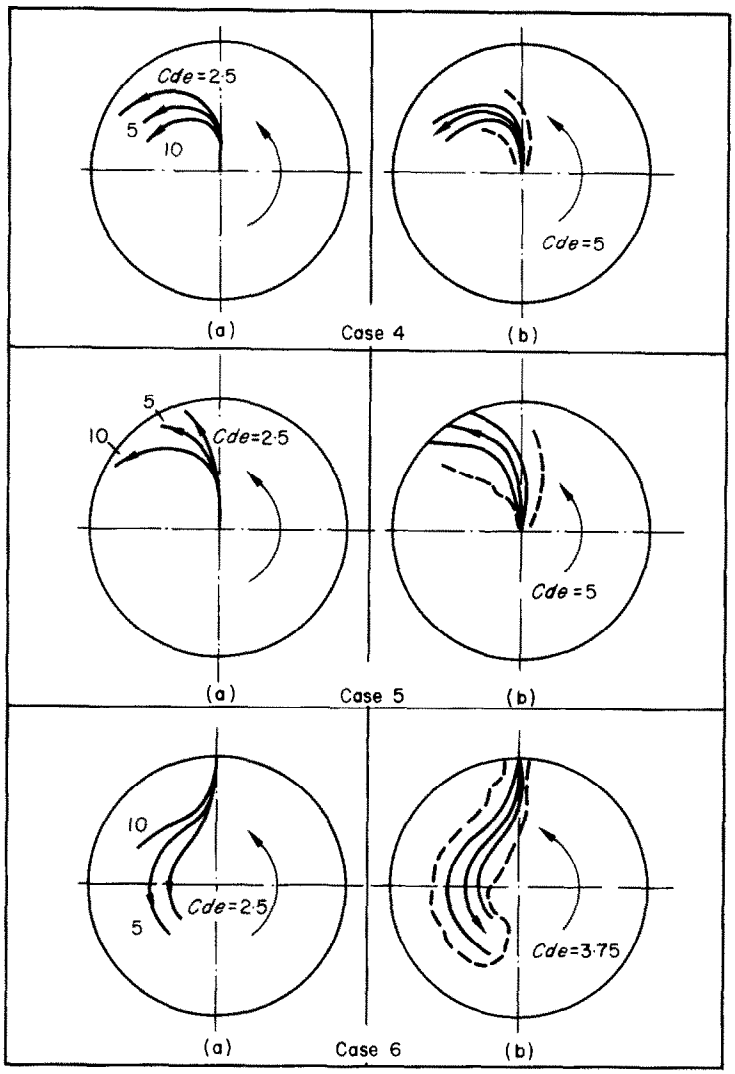

FIG. 8. Calculated and photographed mixing regions of gas oil injections (centre lines on the left are calculated with C_{de} variation, the figures on the right compare the best fitting calculation to the photographed contour given in dashed lines).

Table 1. Data of the spray experiments.

Case No.	1	2	3	4	5	6
Apparatus	mixing chamber	mixing chamber	mixing chamber	photographic engine [12]	photographic engine [12]	photographic engine [12]
Liquid injected	acetone	acetone	acetone	gas oil	gas oil	gas oil
Gas in chamber	nitrogen	nitrogen	nitrogen	air	air	air
Direction of injection	radial inward	radial inward	radial inward	radial outward	radial outward	radial inward
Point of injection from centre of chamber in mm	127	127	127	2	2	76
Nozzle hole size in mm	0·4	0·4	0·4	0·15	0·5	0·35
Injection pressure in kg_f/m^2	290	290	290	125	125	125
Gas density in kg/m^3	1·97	1·49	1·02	5·7	5·7	5·7
Gas temperature in °K	293	293	293	720	720	720
Velocity of flow field	From results of hot wire anometer measurement (near solid rotation)			From [12] based on high speed Schlieren photography		
Recording method	Diffused back illumination			Schlieren illumination		

(b) shows the best fitting centre line with the width of the mixing region superimposed.

The appropriate deflection coefficient is given in the figure. The dashed lines in part (b) of the figure show the mixing region contours taken from the photographs. The deflection coefficients of the best fitting theoretical centre lines vary between 3·75 and 10.

CONCLUSIONS

The theory presented here describes a rather complex phenomenon. Two experimental coefficients and various assumptions are introduced in the formulation to keep the mathematical difficulties involved within reasonable bounds. Not much is known at present about the exact values of the deflection coefficient and the spray width growth coefficient. Thus, additional work is required to enable establishment of correlations for the evaluation of these coefficients. Results of this experimental study being carried out at present at the Technion—Israel Institute of Technology, are to be published in the near future. However, even in its preliminary stage of development, the theory can be applied to calculate the two phase mixing process approximately. In this calculation, values of $C_b = 0{\cdot}22$ and $C_{de} = 7$ are recommended. This is to yield the complete approximate mixing region geometry (centre line, width, penetration) as well as concentration, velocity, temperature and density fields inside that region.

ACKNOWLEDGEMENTS

The authors wish to acknowledge Perkins Engine Co., Ltd., for the grant of a Research Associateship (D. Adler), and for machining facilities for the mixing chamber. They also wish to thank C.A.V. Ltd., for the loan of the high-speed films used in the analysis.

REFERENCES

1. M. M. El Wakil, O. H. Vyehara and P. S. Myers, A theoretical investigation of the heating up period of injected fuel drops vaporizing in air, NACA TN 3179 (1954).
2. F. Eisfeld, Der Einfluss der Luftbewegung auf die Kraftstoffverteilung im Brennraum eines Dieselmotors mit Luftdrehung, Dissertation T.H. Carolo-Wilhelmin, Braunschweig (1960).

3. G. L. BORMAN and JOHNSON, Unsteady vaporization histories and trajectories of fuel drops injected into swirling air, SAE paper 598C (1962).
4. T. DLAUHY and W. H. GAUVIN, Evaporation in spray drying, *Can. J. Chem. Engng* **38**, 113–120 (1960).
5. A. K. BOSÉ and C. T. PEI, Evaporation rates in spray drying, *Can. J. Chem. Engng* **42**, 252–262 (1964).
6. W. E. RANZ and W. R. MARSHALL, Evaporation from drops, *Chem. Engng Prog.* **48**, 141–146 and 173–180 (1952).
7. Y. WAKURI, M. FUJII, T. AMITANI and R. TSUNEYA, Studies on the penetration of fuel spray in a diesel engine, *Bull. JSME* **3**, 123–130 (1960).
8. I. CATTON, D. E. HILL and R. P. MCRAE, Study of liquid jet penetration in a hypersonic stream, *AIAA Jl* **6**, 2084–2089 (1968).
9. G. N. ABRAMOVICH, The theory of turbulent jets, M.I.T. Press (1963).
10. B. E. KNIGHT, Communication to a paper named "The performance of a swirl atomizer", *Proc. Inst. Mech. Engrs* **169**, 104 (1955).
11. R. D. INGEBO, Drag coefficients of droplets and solid spheres in clouds accelerating in air streams, NACA TN 3762 (1956).
12. W. T. LYN and E. VALDMANIS, The application of high-speed Schlieren photography to diesel combustion research, *J. Photogr. Sci.* **10**, 74–82 (1962).

APPENDIX 1

Data Used in the Numerical Investigation of the Equations

(a) *Evaporation function (data for Freon 11 evaporating in helium)*

$\rho_L = 138{\cdot}7$ kg/m^3
$T_g = 348$°K
$P_T = 2{\cdot}5 \times 10^4$ kg$_f$/m^2
$D = 3{\cdot}89 \times 10^{-5}$ m^2/s
$\bar{\mu} = 1{\cdot}458 \times 10^{-6}$ kg$_f$ s/m^2
$C_{pL} = 0{\cdot}208$ kcal/kg °K
$H = 42{\cdot}5$ kcal/kg
$\bar{K} = 7{\cdot}785 \times 10^{-7}$ kcal s/m^2 °K
$\bar{C}_p = 0{\cdot}692$ kcal/kg °K
$\mu_g = 2{\cdot}34 \times 10^{-6}$ kg$_f$ s/m^2
$R_g = 212$ m/°K
$R_{vapour} = 61{\cdot}7$ m/°K
$u_{eq} = 53$ m/s
$d_{mo} = 2{\cdot}5 \times 10^{-5}$ m
$T_{do} = 298$°K
$V_{ro} = 147$ m/s

Saturation pressure coefficients:

$E_0 = 4{\cdot}1 \times 10^{-1}$
$E_1 = 1{\cdot}82 \times 10^{-2}$
$E_2 = 2{\cdot}6 \times 10^{-4}$
$E_3 = 3{\cdot}52 \times 10^{-6}$
E_4–$E_{10} = 0$

(b) *Spray analysis (data for an acetone spray in a nitrogen flow field)*

$c_{mo} = 1$
$T_{eq} = 290$°K
$\Delta T_{mo} = 5$°K
$R_g = 30{\cdot}26$ m/° K
$R_v = 14{\cdot}6$ m/° K
$p = 1{\cdot}86 \times 10^5$ kgf/m^2
$\rho_L = 80{\cdot}6$ kg/m^3
$C_L = 0{\cdot}53$ kcal/kg°K
$C_{pg} = 0{\cdot}248$ kcal/kg°K
$C_{pv} = 0{\cdot}316$ kcal/kg°K
$\alpha = 0{\cdot}045$
$b_o = 2 \times 10^{-4}$ m
$H = 131{\cdot}9$ kcal/kg
$c_b = 0{\cdot}22$
$\phi_{To} = 1$
$\phi_{vo} = 1$

Evaporation function coefficients:

$A_1 = 1$
$A_1 = -2{\cdot}664$
$A_2 = 1{\cdot}051$
$A_3 = 0{\cdot}929$
A_4–$A_{10} = 0$

(c) *Centre line calculation*

Flow field: $u = u_{external} \dfrac{r_{external}}{r}$ (potential vortex).

Evaporation rate: Represented by a density ratio $\rho_g/\rho_v = 0{\cdot}001 + C_\rho\theta$ where $C_\rho = 0{\cdot}016$.

Growth of the spray width: $b = 0{\cdot}00125 + 0{\cdot}0003950\theta$.

Deflection coefficient: $C_{de} = 1$.

Other data common to all the paths are given in the caption of the relevant figure.

APPENDIX 2

Derivation of Equations (13)–(17)

1. *Derivation of equation* (13)

The momentum flux through any two infinite control surfaces, normal to the centre line of the spray, is conserved. If one of the two control surfaces is chosen to pass through the origin of the spray, the other intersecting the centre line at an arbitrary downstream point, the following equation can be written to express the conservation of momentum

$$\int_{-\infty}^{-M_o} u_{eq}\,dm_o + \int_{-M_o}^{+M_o} v_o\,dm_o + \int_{+M_o}^{+\infty} u_{eq}\,dm_o = \int_{-\infty}^{+M} u_{eq}\,dm + \int_{-M}^{-M} v\,dm + \int_{+M}^{+\infty} u_{eq}\,dm. \quad (1.1)$$

Here dm is the mass of a differential element inside the spray and surfaces $-M$ and $+M$ represent the boundaries of the spray.

Subtracting $\int_{-\infty}^{+\infty} u_{eq}\,dm$ from both sides of equation (1.1)

$$\int_{-M_o}^{+M_o}(v_o - u_{eq})\,dm_o = \int_{-M}^{+M}(v - u_{eq})\,dm. \tag{1.2}$$

This equation can be transformed into

$$\frac{4b_o^2}{K_1}\int_{-1}^{1}\Delta v_o v_o \rho_o\,d\xi = \frac{4b^2}{K_1}\int_{-1}^{1}\Delta v v \rho\,d\xi. \tag{1.3}$$

Here $4b^2/K_1$ are the cross sections of the spray, assuming similarity of these cross sections.

The integrands of equation (1.3) are rewritten as follows:

$$\Delta v v \rho = \Delta v(\Delta v + u_{eq})\rho = \Delta v^2 \rho + \Delta v u_{eq}\rho$$

$$= \Delta v_m^2 \rho_{mo}\left[\left(\frac{\Delta v}{\Delta v_m}\right)^2 \frac{\rho}{\rho_{mo}} + \frac{\Delta v}{\Delta v_m}\frac{u_{eq}}{\Delta v_m}\frac{\rho}{\rho_{mo}}\right]$$

Here $v/v_m = f_v(\xi)$ and $\rho/\rho_{mo} = f(\xi, x)$ thus using $u_{eq}/v_{mo} = \alpha$ and the symbols of the integrals given in the notation equation (1.3) takes the following form:

$$b_o^2\,\Delta v_{mo}^2 \rho_{mo}\left(I^o_{vv\rho} + \frac{\alpha}{1-\alpha} I^o_{v\rho}\right) = b^2\,\Delta v_m^2 \rho_{mo}\left(I_{vv\rho} + \frac{u_{eq}}{\Delta v_m} I_{v\rho}\right) \tag{1.4}$$

dividing equation (1.4) by $\Delta v_{mo}^2 \rho_{mo}$ gives

$$b_o^2\left(I^o_{vv\rho} + \frac{\alpha}{1-\alpha} I^o_{v\rho}\right) = b^2 \phi_v^2\left(I_{vv\rho} + \frac{\alpha}{1-\alpha}\frac{1}{\phi_v} I_{v\rho}\right). \tag{1.5}$$

This is a quadratic equation of ϕ_v. Its solution disregarding the minus sign in front of the square root because of physical reasons, gives equation (13) of the paper.

2. *Derivation of equation* (15)

Applying the conservation of injected matter to the control surfaces described in section 1 of Appendix 2 we have:

$$\int_{-M_o}^{+M_o} c_o\,dm_o = \int_{-M}^{+M} c\,dm. \tag{2.1}$$

this equation can be rewritten to give

$$b_o^2 \int_{-1}^{1} c_o \rho_o v_o\,d\xi = b^2 \int_{-1}^{1} c\rho v\,d\xi \tag{2.2}$$

or

$$b_o^2 c_{mo}\Delta v_{mo}\int_{-1}^{1}\frac{c_o}{c_{mo}}\frac{\Delta v_o - u_{eq}}{\Delta v_{mo}}\rho_o\,d\xi$$

$$= b^2 c_m \Delta v_m \int_{-1}^{1}\frac{c}{c_m}\frac{\Delta v - u_{eq}}{\Delta v_m}\rho\,d\xi. \tag{2.3}$$

Division of equation (2.3) by $c_{mo}\Delta v_{mo}\rho_{mo}$ and substitution of $c/c_m = f_c$; $\Delta v/\Delta v_m = f_v$; $c_m/c_{mo} = \phi_c$; $\Delta v_m/\Delta v_{mo} = \phi_v$; $u_{eq}/v_{mo} = \alpha$; $\rho/\rho_{mo} = f_\rho$ as well as the symbols of the various integrals given in the notation yields equation (15) of the paper.

3. *Derivation of equation* (16)

Conservation of heat content applied to the control surfaces of section 1 of Appendix 2 gives for an external gas of constant temperature T_{eq}

$$\int_{-\infty}^{-M_o} T_{eq}Cp_g\,dm_o + \int_{-M_o}^{+M_o} T_o C_L\,dm_o + \int_{+M}^{+\infty} T_{eq}Cp_g\,dm_o$$

$$= \int_{-\infty}^{-M} T_{eq}Cp_g\,dm + \int_{+M}^{+M} TC\,dm + \int_{M}^{+M} Hc(1-\kappa)\,dm$$

$$+ \int_{+M}^{+\infty} T_{eq}Cp_g\,dm. \tag{3.1}$$

Subtracting $\int_{-\infty}^{+\infty} T_{eq}Cp_g\,dm$ from both sides of equation (3.1)

$$\int_{-M_o}^{+M_o}(T_o C_L - T_{eq}Cp_g)\,dm_o = \int_{-M}^{+M}(TC - T_{eq}Cp_g)\,dm$$

$$+ H(1-\kappa)\int_{-M}^{+M} c\,dm. \tag{3.2}$$

Equation (3.2) can be rewritten as

$$\int_{-M_o}^{+M_o}(T_o - T_{eq})\,C_L\,dm_o + \int_{-M_o}^{+M_o}(C_L - Cp_g)\,T_{eq}\,dm_o$$

$$\int_{-M}^{+M}(T - T_{eq})\,C\,dm + \int_{-M}^{+M}(C - Cp_g)\,T_{eq}\,dm$$

$$+ H(1-\kappa)\int_{-M}^{+M} c\,dm.$$

Equation (16) of the paper is derived from equation (3.2) using the definitions of C_{T1}, C_{T2}, ΔT, Δv, α, f_v, f_c, f_T, ϕ_v, ϕ_c, ϕ_T and of the integrals. The derivation involves some algebraic manipulation and the division of equation (3.2) by $\Delta v_{mo}\Delta T_{mo} c_{mo}$.

4. *Derivation of equation* (14)

A mass element of the mixture Δm, contains Δm_g of the external gas and Δm_{L+v} of the injected material. Of this Δm_L in form of liquid and Δm_v vaporized.

$$\Delta m = \Delta m_g + \Delta m_{L+V} = \Delta m_g + \Delta m_L + \Delta m_V \tag{4.1}$$

the concentration is

$$c = \frac{\Delta m_{L+V}}{\Delta m} \tag{4.2}$$

so that

$$\frac{\Delta m_g}{\Delta m} = 1 - c \tag{4.3}$$

the evaporation function is

$$\kappa = \frac{\Delta m_L}{\Delta m_{L+V}} \tag{4.4}$$

thus

$$\Delta m_V = \Delta m_{L+V}(1 - \kappa). \tag{4.5}$$

The volume of this mass element is

$$\Delta V = \frac{\Delta m_g + \Delta m_V}{\bar{\rho}} + \frac{\Delta m_L}{\rho_L}. \tag{4.6}$$

The definition of the spray density is

$$\rho = \frac{\Delta m}{\Delta V} \tag{4.7}$$

so that

$$\rho = \frac{\Delta m}{\dfrac{\Delta m_g + \Delta m_V}{\bar{\rho}} + \dfrac{\Delta m_L}{\rho_L}} = \frac{1}{(1/\bar{\rho}\,(1 - c\kappa) + (1/\rho_L)(c\kappa)} \tag{4.8}$$

$\bar{\rho}$ can be expressed in the following way

$$\bar{\rho} = \frac{p}{\bar{R}T} \tag{4.9}$$

where $\bar{R}$ is the mean gas constant of external gas and vapour.

$$\bar{R} = \frac{\Delta m_g}{\Delta m_g + \Delta m_V} R_g + \frac{\Delta m_V}{\Delta m_g + \Delta m_V} R_v \tag{4.10}$$

this relation can be given the following form

$$\bar{R} = \frac{1 - c}{1 - c\kappa} R_g + \frac{c(1 - \kappa)}{1 - c\kappa} R_v. \tag{4.11}$$

Substitution of $\bar{R}$ into $\bar{\rho}$, and $\bar{\rho}$ into ρ gives

$$\rho = \left\{ \frac{(1 - c\kappa)\left[\dfrac{1 - c}{1 - c\kappa} R_g + \dfrac{c(1 - \kappa)}{1 - c\kappa} R_v\right] T}{p} + \frac{c\kappa}{\rho_L} \right\}^{-1}. \tag{4.12}$$

Finally, substitution of $c = f_c \phi_c c_{mo}$ and $T = T_{eq} + f_T \phi_T \Delta T_{mo}$ yields equation (14).

5. *Derivation of equation* (17)

Equation (17) is derived from Abramovich's ([9] p. 268) basic equation

$$\frac{db}{dx} = c_b \frac{v_m - u_{eq}}{v_{ch}} \tag{5.1}$$

where v_{ch} is a characteristic velocity

$$v_{ch} = \frac{2(\rho_g u_{eq} + \rho_m v_m)}{\rho_g + \rho_m} \tag{5.2}$$

hence

$$\frac{db}{dx} = c_b \frac{(v_m - u_{eq})(\rho_g + \rho_m)}{2(\rho_g u_{eq} + \rho_m v_m)} \tag{5.3}$$

some algebraic manipulations give

$$c_b \frac{dx}{db} = \frac{2}{1 + \rho_g/\rho_m} + \frac{2u_{eq}}{\Delta v_m}. \tag{5.4}$$

The second term of equation (5.4) can be rearranged

$$\frac{2u_{eq}}{\Delta v_m} = 2 \frac{\alpha}{(1 - \alpha)} \frac{1}{\phi_v}. \tag{5.5}$$

Equation (4.12) can be used to express ρ_m, while ρ_g can be expressed using the equation of state

$$\rho_g = \frac{p}{R_g T_{eq}}. \tag{5.6}$$

Thus, the density ratio becomes

$$\frac{\rho_g}{\rho_m} = \frac{T_m}{T_{eq}}(1 - c_m\kappa)\left[\frac{1 - c_m}{1 - c_m\kappa} + \frac{c_m(1 - \kappa)}{(1 - c_m\kappa)} \frac{R_v}{R_g}\right] + \frac{pc_m\kappa}{R_g T_{eq} \rho_L}. \tag{5.7}$$

Here

$$\frac{T_m}{T_{eq}} = \phi_T(\hat{\Theta} - 1) + 1 \tag{5.8}$$

and

$$c_m = \phi_c c_{mo}$$

so that

$$\frac{\rho_g}{\rho_m} = [\phi_T(\hat{\Theta} - 1) + 1]\psi + \frac{pc_{mo}\phi_c\kappa}{R_g T_{eq} \rho_L}. \tag{5.9}$$

Substituting equations (5.5) and (5.9) into equation (5.4) gives after some manipulations, equation (17) of the paper.

L'ÉVAPORATION STATIONNAIRE ET LE MÉLANGE DUN JET DANS UN TOURBILLON GAZEUX

Résumé—On établit et illustre par de nombreuses expériences une théorie pour le calcul de l'évaporation stationnaire et du mélange d'un jet liquide dans un tourbillon gazeux. Cette théorie est basée sur la mécanique des milieux continus plutôt que sur la théorie d'une goutte isolée permettant ainsi la considération de l'interaction entre les gouttes à l'intérieur du jet.

On peut calculer le trajet du jet, le taux d'évaporation aussi bien que les champs de vitesse, de concentration et de température.

Les équations résultantes doivent être résolues numériquement. On donne la procèdure numérique ainsi que les résultats numériques.

DIE STATIONÄRE VERDAMPFUNG UND VERMISCHUNG EINES STRAHLS BEI GASVERWIRBELUNG

Zusammenfassung—Es wird eine Theorie erläutert für die Berechnung der stationären Verdampfung und der Mischung von einem flüssigen Strahl in einem gasförmigen Wirbel. Die Theorie wird durch einige Experimente bestärkt. Diese Theorie basiert mehr auf der Betrachtung eines Kontinuums als auf der Betrachtung von einzelnen Tropfen. Dadurch wird die gegenseitige Beeinflussung der Tröpfchen besser berücksichtigt.

Der Weg des Strahls, die Verdampfungsgeschwindigkeit, und die Konzentrations-, Geschwindigkeits- und Temperaturfelder können berechnet werden.

Die sich ergebenden Gleichungen müssen numerisch gelöst werden. Die Berechnungsprozedur und eine numerische Untersuchung der Gleichungen werden diskutiert.

СТАЦИОНАРНОЕ ИСПАРЕНИЕ И ПЕРЕМЕШИВАНИЕ КАПЕЛЬНОЙ СТРУИ В ГАЗОВОМ ВИХРЕ

Аннотация—Описывается и подкрепляется экспериментально теория расчета стационарного испарения и перемешивания жидкой струи в газовом вихре. Эта теория основывается больше на теории сплошных сред, чем на теории единичной капли, что делает возможным рассмотрение взаимодействия между каплями в струе.

Можно подсчитать траекторию струи, скорость испарения, также как и поля концентрации, скорости и температуры.

Выведенные уравнения должны решаться численно. Обсуждается методика расчета.